

# Matchsticks, Scramjets, and Black Holes: Numerical Simulation Faces Reality

Elaine S. Oran\*

Naval Research Laboratory, Washington, D.C. 20375

**The evolution of the science and art of numerical simulation of complex, complicated fluid flows has made enormous strides in the past 40 years. We have progressed from relatively simplified one-dimensional steady-state results to fully three-dimensional, time-dependent simulations including very complex physics. These advances have been driven by new computational hardware, new algorithms for solving the equations, and the real need for this technology. The broad range of applications that are possible are emphasized and some of what we can now do, what we have learned, and where we might go with this exciting technology in the future is described.**

## I. Introduction

**T**HIS paper and lecture are dedicated to Hugh L. Dryden. He was a brilliant researcher and a determined administrator, and he was truly dedicated to the defense of our country and access to space. He had a deep appreciation of the importance of both the basic, underlying, often controlling physical mechanisms and their application to practical engineering problems.<sup>1</sup> Given the span of his life, 1898–1965, he may have had a glimmer of the consequences of the growth of computer technology and simulation capabilities and their multifaceted applications to so many fields of science and engineering. Nevertheless, I think that I can make a case that he would appreciate both what has been done and what is left to do.

There are a number of themes in this paper, all following from a central, key observation concerning the work done today in numerical simulation of fluids. This observation is that *numerical simulation of real problems now involves not only fluid dynamics, but requires combining knowledge and methods from many disciplines*. For example, by computational fluid dynamics (CFD), we commonly mean not only fluid dynamics, but a multidisciplinary field involving science (physics, chemistry, biology), mathematics (applied mathematics and numerical analysis), and engineering (aerospace, mechanical, civil, chemical), all linked with principles of computer science and engineering. We call this multidisciplinary approach *numerical simulation of complex flows*.<sup>2</sup>

Many of these flows are reactive, where “reactive” here has several meanings. First, many involve a variety of different interacting chemical, atomic, biological, or even nuclear species. Many, however, are reactive in a different sense: They are highly interactive, in that they react very strongly, that is, nonlinearly, with their surroundings, either with concurrent processes (such as electromagnetic radiation or thermal conduction), the geometry of their space, or the composition of their boundaries. Numerical simulation of these complex, complicated flows gives us a way to combine very different kinds of physical processes and then use the results to teach us how things work, test theories, and even design systems. It shows the importance of understanding fundamental interactions that are generally applicable to a broad range of problems. The simulations can describe systems that differ by many orders of magnitude in spatial and temporal timescales, but all of these systems may be represented by a very similar mathematical formulation. Taken together,

this thrust in numerical simulation of complex flows pushes the limits of computer science and technology and is a major driver for expanding our capabilities in these fields.

Now we begin by going through a series of examples of truly state-of-the-art computations. These are only representative, not in any way inclusive, of the tremendous amount of work now being done, all around the world. Each example will be used to make a specific point or two, and unfortunately, each is described here only briefly. They do, however, give a sense of the breadth of the effort. Let us start, moving from under the sea, to the land, to near space, to the sun, to the stars, and beyond.

## II. Rather Quick Trip Through the Universe

The collection of Figs. 1–11 is taken from a variety of numerical simulations describing scenarios from under the sea to far outer space. These are three-dimensional unsteady computations with complex geometries and flow structures, complicated physics including energy-releasing chemical, atomic, or thermonuclear reactions, various types of physical diffusion, multiphase effects, and electromagnetic radiation.

Figure 1 is taken from a simulation of the oscillating and distorting fin of a small tropical Pacific fish, the bird wrasse,<sup>3</sup> which can move quite efficiently against a 5-kn current. Figure 2 is from a simulation of a torpedo being launched from a submarine,<sup>4</sup> a complicated flow that involves separating and moving bodies. Then moving to the air–sea interface, Fig. 3 is from a simulation of a DDG51, a Naval destroyer, moving at 20 kn. The ship is modeled complete with gases coming from the smoke stacks and a helicopter that must land on the aft deck.<sup>5</sup>

Next are simulations of land-based transportation. Figure 4 is a simulation of the Shinkansen, the bullet train, entering a tunnel.<sup>6</sup> Shock waves form as the train moves through the tunnel. Figure 5 is from a simulation of an automobile being crushed, as would have occurred during the explosion in Toulouse (V. N. Gamezo, private communication). Then we move to simulations of a series of phenomena that can play havoc with our lives: fires and explosions<sup>7–9</sup> in Fig. 6, which are complicated phenomena involving fast fluid flows and intense energy release; the not-so-innocuous hornet<sup>10</sup> in Fig. 7; and winds carrying contaminants in the region of the Pentagon, Route 395, and the Fashion Center<sup>11</sup> in Fig. 8.

There are simulations of phenomena occurring on much larger scales. Simulations of flows around space capsules reentering the Earth’s atmosphere,<sup>12</sup> as shown in Fig. 9, allow us to determine the best configuration for their reentry. Simulations of solar eruptions and flares,<sup>13</sup> as in Fig. 10, allow us to understand, predict, and even protect ourselves and equipment against changes in space weather. Finally we turn our attention to far outer space and the stars. There are simulations of thermonuclear supernovas<sup>14</sup> in Fig. 11, the “standard candles” that we use to compute astronomical and cosmological distances, as well as the rate of expansion and curvature of

Presented as Paper 2002-0001 at the 40th Aerospace Sciences Meeting, Reno, NV, 15–18 January 2002; received 19 March 2002; revision received 2 April 2002; accepted for publication 2 April 2002. This material is declared a work of the U.S. Government and is not subject to copyright protection in the United States. Copies of this paper may be made for personal or internal use, on condition that the copier pay the \$10.00 per-copy fee to the Copyright Clearance Center, Inc., 222 Rosewood Drive, Danvers, MA 01923; include the code 0001-1452/02 \$10.00 in correspondence with the CCC.

\*Senior Scientist for Reactive Flow Physics, Laboratory for Computational Physics and Fluid Dynamics, Code 6404; oran@lcp.nrl.navy.mil. Fellow AIAA.

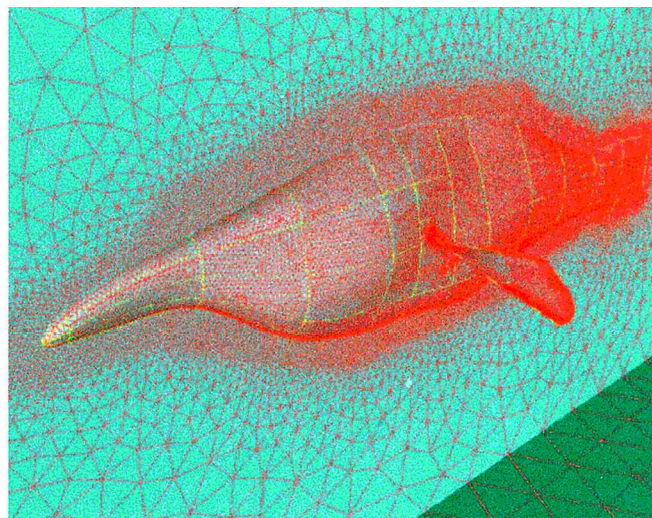
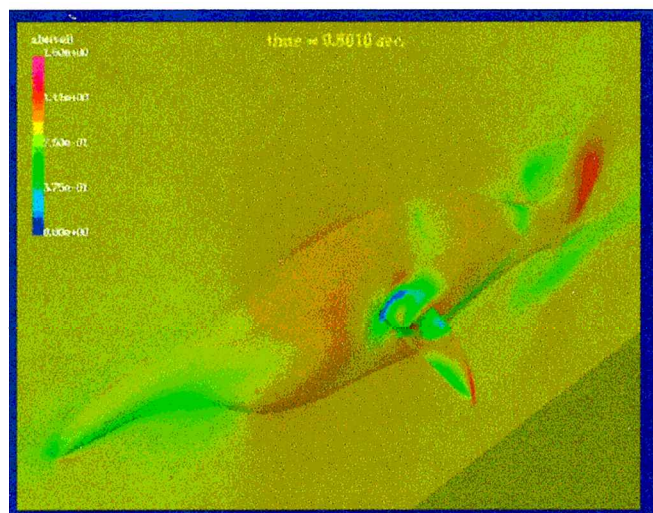


**Fig. 1** Flow around the tropical Pacific fish, the bird wrasse,<sup>3</sup> with its oscillating and deforming fins, shows the importance of the time dependence of the deforming fins to its propulsion. This wrasse can move efficiently against a 5-kn current. Right, surface mesh and meshes on a vertical plane through the center of the fish. Left, absolute value of the velocity on the surface and a plane through the centerline.

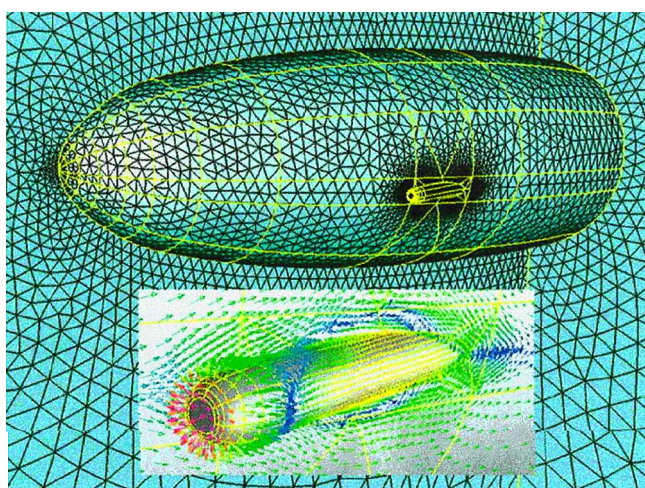


**Fig. 2** Torpedo launch from a submarine bay.<sup>4</sup> Flow complications arise as water moves into the bay when the torpedo is launched, as flow is induced by the relative motion of the submarine and the torpedo and due to the effects of the water jet used to propel the torpedo. Background, surface mesh and mesh through the central plane. Inset, closer view of torpedo showing velocity vectors.

the universe. Now consider some of the general properties of these particular calculations.

### Geometrical Complexity

Most of these simulations are geometrically complex. For example, the simulations of the wrasse, submarine and torpedo, DDG51 destroyer, bullet train, automobile, hornet, Pentagon, and reentry capsule all have complicated, internal and external boundaries. The wrasse and hornet are further complicated by moving fins and wings, respectively. The wrasse simulation is even further complicated by the fact that the wings deform as they move. The torpedo launch is complicated by flow physics introduced by separating bodies.

Representing bodies that move, distort, and react with the flow and other bodies requires special techniques for representing the geometry. The simulations of the wrasse and the submarine with torpedo used “unstructured” grids, in which the computational grid (making up the computational “cells”) were made up of triangular elements. The simulations of the ship and the Pentagon used grids of square and rectangular elements, with special algorithms to describe those cells through which the body passes.

The train and reentry capsule used structured “body-fitted” grids that combined different types of elements. The simulation of the automobile is a hybrid: An unstructured grid of triangular elements is used to represent the material of the car, and a “structured” Cartesian grid with cut cells describes the background flow.

Finding a suitable grid to represent a complicated three-dimensional geometry has always been a roadblock in CFD. Over the past 25 years, enormous human and computational resources have gone into developing methods for describing such complex geometries. The examples shown in Fig. 1 use only a few of the many different approaches attempted so far (many of these are summarized in Ref. 2, Chapter 6). An important conclusion of all of this work is that there is an enormous benefit to be gained by intelligently gridding space.

### Physical Complexity

Many of these simulations involve complex physical processes in addition to fluid dynamics. The automobile crash involves gas-surface interactions and required combining computer programs that solve solid mechanics and gas-phase fluid dynamics. These involved equations of state for car metal, rubber tires, and glass windows, each of which responds differently to shocks and stress. The deflagrations involve a complex sequence of gas-phase chemical reactions, sometimes forming soot and particles. In addition to fluid dynamics to compute the plasma flow, the simulation of the solar eruption includes descriptions of the behavior of the electric and magnetic fields needed to compute the reconnecting magnetic field lines. The thermonuclear supernova involves a gravitational field that varies from zero gravity at the center (0 cm) to about  $5 \times 10^6$  times Earth gravity at the outer edge ( $10^8$  cm) of the star, and a complex series of nuclear interactions that transforms  $^{12}\text{C}$  and  $^{16}\text{O}$  into a series of heavier elements such as neon, magnesium, silicon, and up to nickel.

### Flow-Structure Complexity

Most of these simulations develop extremely complicated flow-fields, containing, for example, shock waves, steep density gradients, and regions where there is rapid energy release and fluid expansion. These local changes in the flow may occur over distances that are small compared to the size of the system, they might appear suddenly and then become dissipated in the flow, or they might move at different velocities through the system. It is necessary to capture the event, resolve it with a relatively small grid, and ensure the event is computed properly even if it moves. In these cases, special grid refinement techniques are used. All of the computations shown in Figs. 1–11 use some form of grid



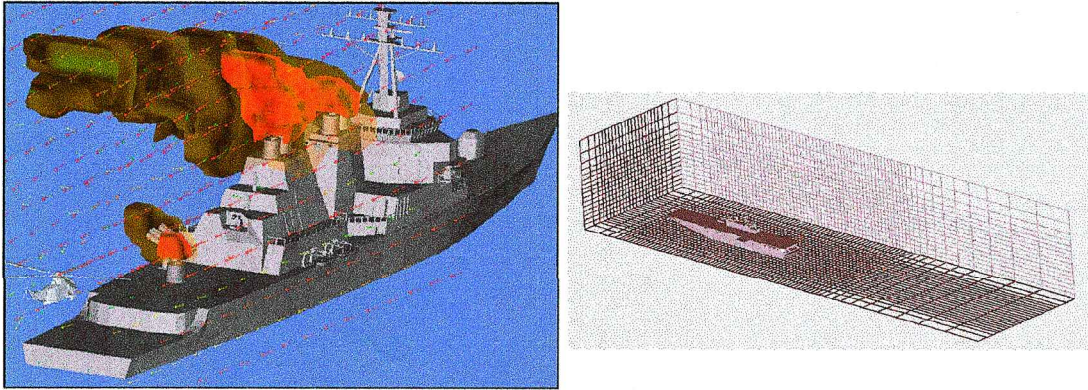


**Fig. 3** Naval destroyer, a DDG-51, moving at 20 kn with a 20-kn headwind, with smoke from the stacks and an approaching helicopter with rotating blades.<sup>5</sup> Wind and smoke passing over the ship create rapid background fluctuations in which a helicopter must land. Simulations were used to create background airflows for virtual reality training for helicopter pilots and to design deflectors to keep the gases out of open bays. Note use of a Cartesian grid and special methods to embed non-Cartesian structures and moving helicopter blades. Left, velocity vectors and right, grid.

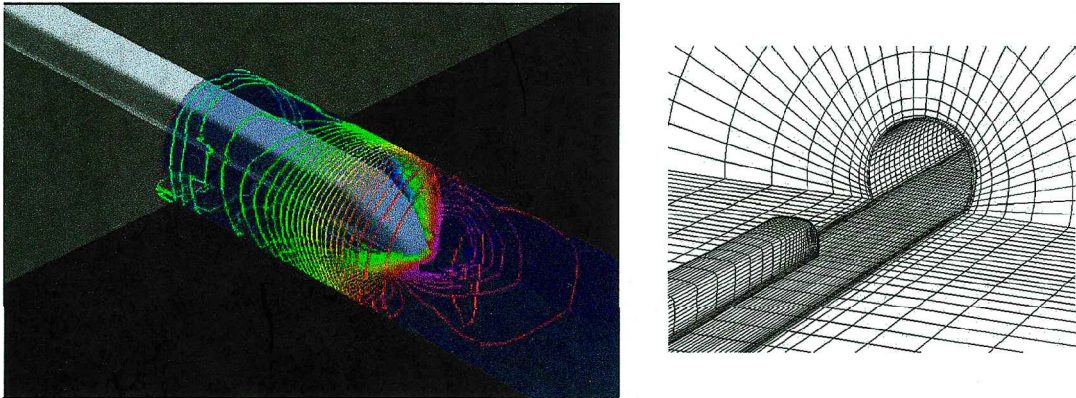


**Fig. 4** Shinkansen, or bullet train, entering and traveling through a tunnel.<sup>6</sup> The Shinkansen now runs at 300 km/h (roughly Mach 0.25). Future trains will run over 550 km/h. As they go through tunnels, the increased pressure as the train enters the tunnel creates a compression wave that can become a shock wave, creating sonic booms and shaking and potentially damaging houses. Simulations are used to test train and tunnel modifications for minimizing shock effects. Left, contours of pressure around a train entering a tunnel. Right, overset body-fitted grid.

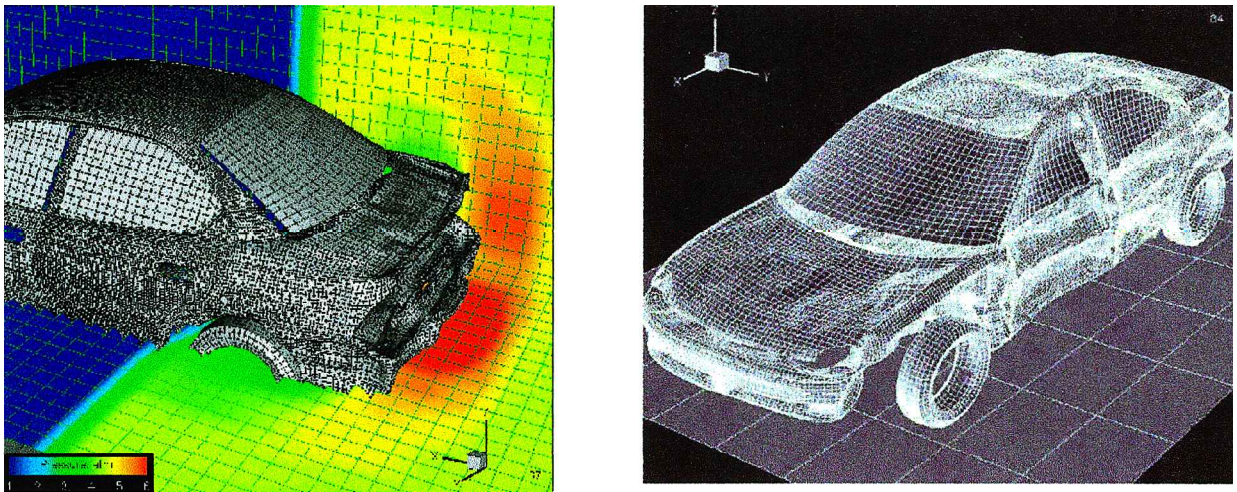


**Fig. 5** Strong blast hitting and crushing an automobile (V. N. Gamezo, private communication) shows the vulnerability of the vehicle to impact (e.g., blast from ammonium nitrate explosion in Toulouse in September 2001). Calculation combines a Cartesian gas-phase fluid code (FAST3D, used to compute flow) and an unstructured structural-mechanics code, DYNA3D that includes material properties of metal (car frame), rubber (tires), and glass (windows). Left, blast halfway through car, pressure (shown by colors). Right, grid on car and selected planes.

refinement and adaptation. For example, the computational grid around the wrasse consists of elements that move and reconnect as the fin oscillates. The grid around the Shinkansen moves with the Shinkansen. The grid describing the eruptive solar event has rectangular blocks of finer, square cells in regions where the ratio of the electric current to the magnetic field is high. The use of local, adaptive grid refinement will come up again later in this paper.

#### Predictive and Design Capabilities

Some of these simulations show us how to improve or design propulsion or aerodynamic systems. The propulsion of the bird wrasse teaches us how the wrasse uses its pectoral fin to produce strong, forward motions that allow this small fish to swim against strong currents. The flow over the DDG51 both shows us how to optimize the design of the aft deck to account for aerodynamic effects and provides flowfields used to train helicopter pilots to land



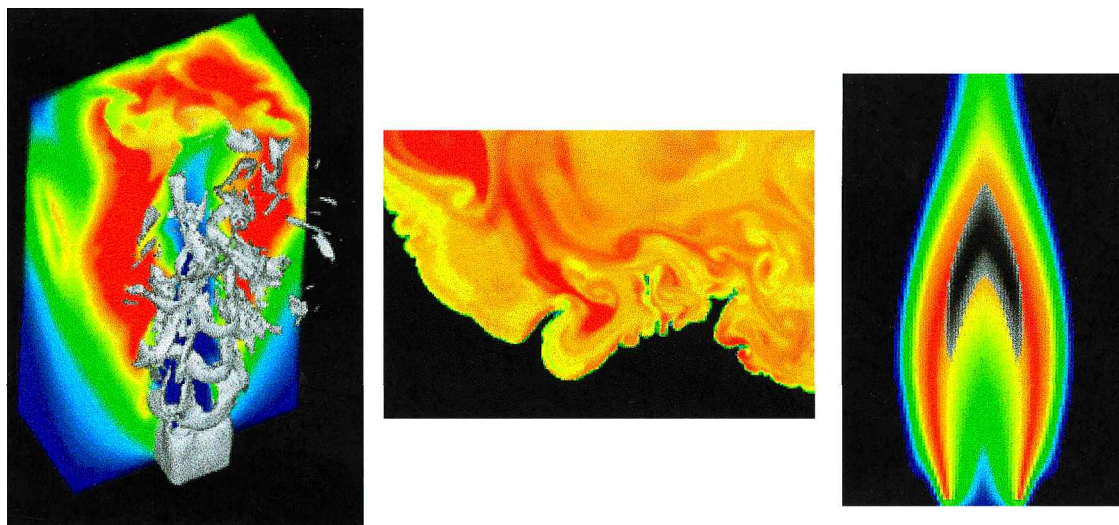


Fig. 6 Deflagrations and detonations involve compressible fluid dynamics, fast energy release, and diffusive or radiative processes. Left, diffusion flame,<sup>7</sup> with vorticity in gray and temperature shown by colors. At the end of each up and down stroke, vortices are shed by twisting the wing. This generates lift and thrust. The grid is an unstructured mesh with an overset grid. Center, turbulent premixed flame in system about to detonate.<sup>8</sup> Right, laminar, sooting diffusion flame; colors are temperature.<sup>9</sup> Black in the center of this flame is a region of heavy sooting.

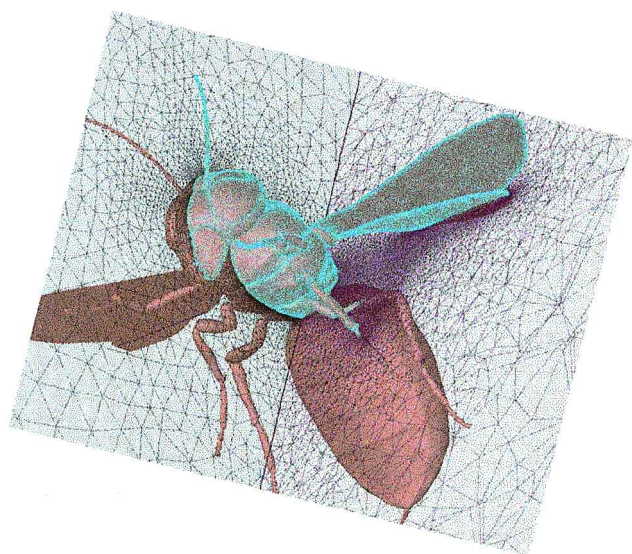


Fig. 7 Hornets fly by flapping their wings.<sup>10</sup> For a hornet, the flapping frequency is about 100 Hz, and the Mach number is about 0.12 (6 m/s). At the end of each up and down stroke, vortices are shed by twisting the wing. This generates lift and thrust. The grid is an unstructured mesh with an overset grid.

safely. The simulations of the bullet train teach us how to design and position the trains to minimize the annoyance and discomfort of shocks created by trains passing through tunnels. The simulation of the reentry capsule shows us how to stabilize and preserve the capsule by adjusting the angles of attack when it reenters the atmosphere.

The sum of what is shown in Fig. 1–11 gives us powerful predictive and design capabilities. Interactions of gases from exhaust stacks and winds, and with the flow around the surface of the ship, give us a way of estimating how structural features of the ship affect fluctuations in the background air. The interactions of the car and the background shocked flow give us a way of estimating how the car will respond to shocks and collisions. The movement of contaminants through a city gives us a predictive capability that we can use to guide our escape from and evaluate danger zones from the release of biological agents. Simulations of solar eruptions can be used to predict the consequences of these events on space and communication systems.

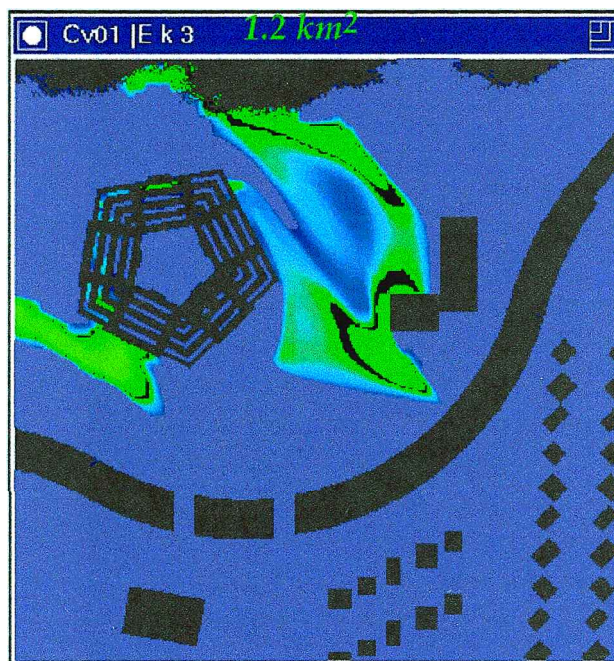


Fig. 8 Release (lasting 30 s) of an agent near the Pentagon, moves in a background wind at 1 m/s from the northwest. Trees, geometries of buildings, highways, and terrain affect movement and deposition of agent.<sup>11</sup> Density of an agent in a horizontal plane close to the ground level of the Pentagon is shown.

#### Basic Scientific Knowledge

In addition to prediction and design, the simulations provide insight into more fundamental physical mechanisms that are common to a wide range of problems. For example, flames and explosions are crucial elements of engines (such as automobiles, scramjets, or ramjets), explosives and propellants, shaped charges, and weapons systems. In all of these applications, safety and efficiency are critical. Simulations of flames and explosions give us understanding of how these phenomena actually work, which in turn provides insight into ways of controlling and using them. Basic simulations of flames and detonations can be carried out for the carbon-oxygen chain of nuclear reactions found in thermonuclear supernovas. Such explosions are the source of heavier elements that are then distributed throughout the universe. The signatures of these supernovas, the electromagnetic spectra



emitted during and after the explosion, are so uniform throughout the universe that they are used as standard candles by which expansion rates, curvature, and even the age of the universe are measured.

Solution Process

An overview of the entire process involved in producing the simulations shown in Figs. 1–11 is given in Table 1. The first step is determining an appropriate model of the physical system. This is usually a set of coupled, partial differential or integral equations for variables that change in time and space. The next step involves deciding on which numerical algorithms to use to transform the model equations into a set of coupled algebraic equations. The third step is actually writing a computer program to solve these algebraic equations. This requires deciding on a data structure and internal

procedure in the program. It is where the representations of the problem meet the limitations of the actual number crunching process. The last step requires dealing with all of the numbers that actually come out of the computer calculation.

Each of these steps, and every intermediate step not listed in Table 1, appears to be a step further away from reality. The model equations only represent the reality. The algebraic equations constituting the numerical algorithms are one of many possible (and legitimate) representations of the equations. The computer program, the data structure, and the order of operations have the possibility of introducing even other differences. Then we are limited by what we look at and how we look at the numerical results produced. With all of this, it is amazing how well the simulations shown in Figs. 1–11 reproduce the major features of the problems they are solving.

III. Some General Observations

The examples shown span over 10 orders of magnitude in size. They involve various types of complexity, such as complicated and changing geometries, chemical, atomic, or nuclear reactions, diffusion processes, electromagnetic fields and radiation, or multiphase interactions. Yet, when we write down the various sets of equations to describe the different problems, there is an amazing similarity in the underlying forms of the equations. This seemingly trivial (and lucky) point is at the heart of what has allowed us to

Table 1 Computational procedure	
Process and representation	Caveat
The Real World	
Define model equations	Equations are an approximation of the real problem
Determine numerical algorithms suitable for transforming the equations into algebraic form	Algorithms are an approximation to the model equations
Program the algorithm for a computer	The computer implementation is an approximation to the algebraic equations
Analyze and present results in the form of graphs, movies, etc.	These show selected interpretations of the result
Four (at least) steps removed from the real world, but hopefully the important features are reproduced.	

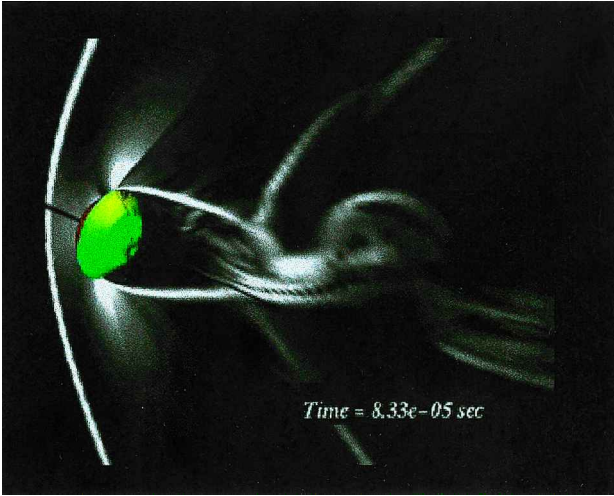


Fig. 9 Simulations of the stability during the reentry dynamics of the MUSES-C space capsule,<sup>12</sup> here at Mach 1.3. (Project start in 1995, satellite launch in 2003, rendezvous with asteroid Nereus in 2004, return by a capsule that detaches from the mother spacecraft in 2007.) Simulations show recirculation zone and the recompression shock behind the capsule. Density gradients in gray, stronger gradient is lighter gray, and capsule in green.

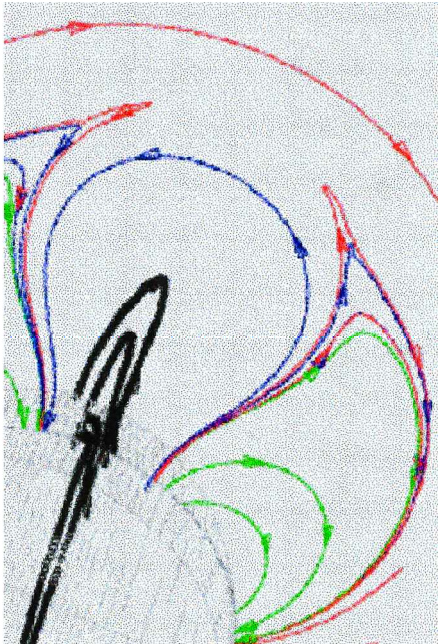
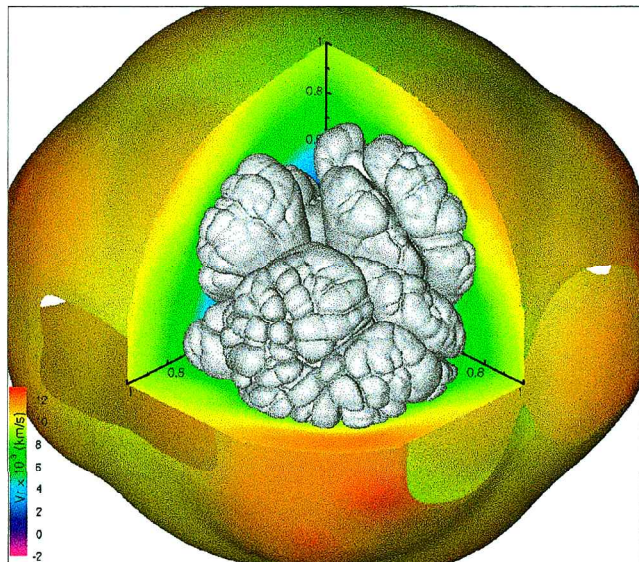
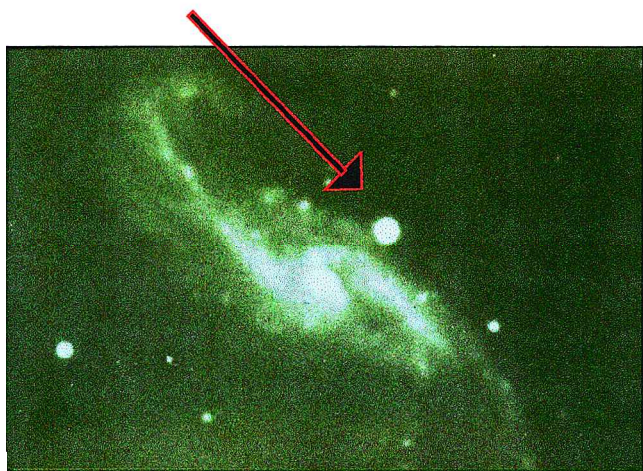


Fig. 10 Solar eruptions and flares.<sup>13</sup> Left, LASCO image taken during the 1997 solar eruption; inner speckled orange image is the sun in wavelength of helium ultraviolet; outer image is white light scattered from the corona. Right, frame from MHD calculation showing structure and reconnection of magnetic field lines. Colors represent different flux systems: Black lines are stretched along the surface by local nonuniform rotation that builds stress into the magnetic field.





**Fig. 11** Type Ia supernovas, the universal standard candles, release about  $10^{51}$  ergs in 2 s and convert  $^{12}\text{C}$  and  $^{16}\text{O}$  to higher elements. Left, observation of galaxy NGC4536 with arrow pointing to explosion of SN 1981B. Right, taken from simulation of predetonative stages of a generic type Ia. Gray surface is the turbulent flame front.<sup>14</sup> Background color is radial velocity.

advance as far as we have in our attempts to find solutions to hard problems.

All of the sets of governing equations can be written in one form, that of a generalized continuity equation for  $\rho$ :

$$\frac{\partial \rho}{\partial t} + \nabla \cdot f(\rho) = S$$

where  $\rho$  is a vector comprising a group of conserved quantities (such as density, momentum, and energy). Here  $S$  is a source or sink of  $\rho$ , and  $f$  are the fluxes of  $\rho$ . Depending on what  $\rho$  is, this equation has other names: the Euler equations, Navier–Stokes equations, reactive-flow conservation equations, or equations of multiphase flow. Because of the similarity in the forms of the equations, the same algorithms and methods for coupling different algorithms can be applied across many fields to represent physics over many scales.

It is only natural to ask, Why is this form so generally valid? One answer is that  $\rho$ , which is usually density, momentum, and energy, is a conserved physical quantity. Then as long as these quantities are reasonably smooth in space, we can write down this equation, which says the following: As a conserved quantity that moves from here to there, it must pass through all of the points in between. Then the physical conditions are conservation, causality, and enough molecular collisions to be able to assume that the fluid is in equilibrium, so that the macroscopic equation written above is valid.

This explanation, though physically intuitive, seems almost too obvious and off handed, the kind of statement that usually calls for careful questioning. Looking into it more deeply, we see that this explanation is actually a statement of basic physics that is well founded in kinetic and fluid theory. The form of the generalized continuity equation can be derived by assuming assemblies of atoms and molecules, assuming enough collisions to obtain equilibrium in a volume of fluid, and taking the appropriate averages and integrals over quantities to obtain their mean values of these conserved quantities over a volume of space. Thus, it is possible to go from basic concepts of atoms and molecules colliding and reacting to derive the sets of equations represented by a continuity equation.

The continuity equation has several qualitative physical properties that should be summarized here. One of these properties is causality: The material currently at a given point arrives there only by previously leaving another place and passing through all intermediate points. Another property is conservation: The total quantity of  $\rho$  in a closed system without source or sink terms does not change. A third property is positivity: If the convected quantity  $\rho$  is originally positive, it will never become negative due to convection alone. Finally, the continuity equation is also time reversible: Changing  $t$  to

$-t$  and  $\mathbf{x}$  to  $-\mathbf{x}$  leaves the equation unchanged. Galilean invariance is a related property that states that the laws of physics are the same in all inertial systems and so must be independent of the coordinate system in which they are observed.

At this point it is worth a small digression back to the discussion of Table 1, specifically, to the issue of numerical representations of the continuity equation. Before it is solved on the computer, we must use some numerical algorithm to recast the equation into an algebraic form. To the extent possible, we would like the numerical algorithms to reflect these properties of causality, conservation, positivity, time reversibility, and Galilean invariance. When algorithms are not conservative, we find unphysical instabilities or growing errors in the solution. Many of the common and annoying problems that arise in the solution of continuity equations occur because the quantities become unphysically negative. Time reversibility is sometimes mirrored in the numerical methods, but it is usually ignored because even a small amount of numerical error breaks this symmetry. Galilean invariance is difficult to include exactly because the use of any grid imposes, in effect, a preferred coordinate system on the numerical solution. The better numerical algorithms tend to confine errors associated with different frames of reference to short wavelengths and small amplitudes.

There is another observation that can be made about the simulations that provides an important link to Hugh Dryden's work and philosophy. To understand what is happening in very complex three-dimensional flows, we need to understand the simpler, more general processes occurring in the flow. For example, to understand the flow in the area of the Pentagon, you must at least understand what happens when a flow passes over a cube, a pentagon, then perhaps the Pentagon. We use simpler simulations to study important parts, and parts of these parts, and syntheses of many parts. These more elementary or fundamental simulations have implications for broad classes of systems. Consider the flame and explosions example shown earlier. Flames and their transition to detonations are elements in explosions in chemical plants, propulsion, weapons design, and supernovas.

#### IV. Several Case Studies

By simulating such a wide range of physical systems, we have accumulated a large body of practical knowledge concerning how best to approach a new type of problem, deal with physical and geometrical complexity, trust (and mistrust) input data, trust (and mistrust) the answers, and learn something useful from simulations that may not yet (ever?) be perfect. We have learned the value of diagnostics, particularly graphical representations of large amounts of data. We have learned the importance of understanding, and

perhaps even controlling, the fundamental components of a flow. Finally, we have learned that sometimes we have to pay particular attention to the dynamics of a flow, which means that to understand what is happening, we actually need to observe how it evolves.

Now let us illustrate these points by describing several of the examples in Figs. 1–11 in some detail, this time moving from the sun toward the Earth and perhaps back out. We consider the eruptive flare with a mass ejection from the sun, a contaminant flow through an area similar to the Washington Mall, and an element of a problem common to many peaceful, hazardous, and military scenarios, a flame becoming a detonation.

### Solar Storms

Coronal mass ejections and eruptive flares are large, energetic, dynamic events that drive space weather and geomagnetic disturbances and that follow the solar cycle. They involve some sort of triggering mechanism that destroys the equilibrium of the corona, allowing the magnetic field to erupt outward and eject plasma into the heliosphere. After this ejection, the magnetic field reconnects and settles down to a new equilibrium.

The Large Angle and Spectrometric Coronagraph (LASCO) is an instrument on the Solar and Heliospheric Observatory (SOHO) satellite, launched in 1995. LASCO contains three coronagraphs that image the solar corona from 1.1 to 32 solar radii. (The idea of a coronagraph is to block light coming from the solar disk so that it is possible to see the relatively faint emission from the solar corona.) Figure 10 contains two pictures: The one on the left is an image taken by LASCO in 1997 during a solar eruption. The inner part of the speckled solar disk shows the sun in the wavelength of helium ultraviolet. The region surrounding this is white light scattered from corona, and it is believed that this is showing the structure of the magnetic field lines. The right side of Fig. 10 is a part of a magnetohydrodynamics (MHD) calculation that shows the dynamics and structure of magnetic field lines and magnetic reconnection of these lines.<sup>13</sup>

Figure 12 shows a series of frames from a numerical simulation of such an event.<sup>15</sup> These are results from a three-dimensional, unsteady MHD simulation, which includes a full description of the behavior of the plasma fluid, magnetic, and electric fields. Initially, a strong displacement of the quadrupolar magnetic field is imposed locally in the photosphere in a region around the solar equator (Figs. 12a and 12b). As a result of this shear, the magnetic field lines near the surface are distorted and expand outward (Figs. 12c and 12d), and the outlying fields, of opposite polarity, are also pushed out (Fig. 12d). Field lines reconnect (Fig. 12e), forming magnetic flux ropes (Figs. 12f–12h), the now loosely restrained flux erupts (Figs. 12h and 12i), and magnetic field and plasma are eventually blown out into interplanetary space (Figs. 12j and 12k). Finally, the field lines anchored in the sun then reconnect, reform, and the system equilibrates (Figs. 12k and 12l). In the calculation, the time building up to the ejection is about 8 h, somewhat less than the few-days time it takes in real events. The ejection process itself, however, takes about 2 h, which is about what is observed.

This is an amazing calculation in several ways, and it illustrates many of the points we wish to make in this paper. From the point of view of physics, it is an extremely complicated calculation showing magnetic field lines moving, interacting, and reconnecting, leading to large-scale plasma ejections from the sun. The computation required highly accurate algorithms to solve the appropriate forms of the coupled continuity equations, now containing descriptions of the dynamics of electric and magnetic fields. The geometry of the system is not complicated initially, but the flow and magnetic field structures become complex and change dramatically in time. The calculation, therefore, required an algorithm for adaptive grid refinement, in this case one that used several levels of superimposed blocks of increasingly finer computational elements. This calculation is the culmination of an enormous amount of previous work on the dynamics and interactions of solar magnetic fields. It is also the culmination of an enormous amount of previous work on numerical algorithms for fluid dynamics, MHD, and representing the structure of complex evolving flows and fields.

### Contaminant Flow Through Cities

A terrorist release and the subsequent spread of a biological agent, such as anthrax, is a current major concern for civil defense. These agents may be droplets, particles, vapor, or gases. They may spread quickly through an urban area, and they are strongly affected by prevailing winds, the large- and smaller-scale local geometry imposed by the buildings and terrain, the presence and the seasonal variation of foliage, and the time of day due to solar heating and local traffic. Because of the importance of this problem, extensive efforts have been made to create realistic, reliable models of flow in urban areas. Two of the most important questions are as follows: How far do these agents spread? How quickly?

Figure 13 shows two frames from a simulation of a particle release in an urban area  $1.5 \times 1.5 \times 0.4 \text{ km}^3$ , modeled after the Washington Mall.<sup>16,17</sup> The view is from the southwest, and the wind is coming from the east at 3 m/s. The area shown is resolved to 5-m resolution in each direction on a stretched Cartesian grid, using special algorithms to represent curved surfaces in the computational domain. The colors represent the mass density of the agent.

Particles, released in the eastern corner at ground level, are caught in the wind and carried downstream. Flow over and around the buildings generates vortices, leading to fluctuations in the flow that strongly affect the sideways spreading. Thus, as the particles move downstream, they are caught in the recirculation regions between buildings. Heating and cooling, due to the local change in temperatures caused by shadows or automobile emissions, affect how the particles spread. Trees and their foliage, and consequently the time of year, are also important.

The major and fortunate conclusion of the extensive simulations that have been performed is that simplifications are possible and that the spread of agent can be predicted. This reassuring result derives from the observation that the geometry is a major controlling factor in how the agent spreads. Buildings trap agents in recirculation zones created by vortices that are shed when the wind blows over them. The agents escape from the vortices at a small percent for each vortex rotation, resulting in an exponential decay of the local density of the agent. The coefficient in the exponential decay depends on the geometry, the time of day, and the wind speed and fluctuations, all information that we can take into account ahead of time. Because of this, if a location has been calibrated, there is no need to do ensemble averages to predict the results. Finally, the computations suggest that, close to the source of the agent, the size of the contaminated area is not very sensitive to the exact amount of agent released. This is not true downstream, where the danger is proportional to the amount released.

This is a very complex simulation that includes models of many kinds of physical and chemical processes and uses new techniques to represent the geometry of complex terrain. Such complicated computed flows are really too complex to understand on their own. The understanding that leads to confidence in this simulation is based on many years of computations that have led to this capability. For example, important information is contained in the relatively simpler calculations of a viscous flow over obstacles in a channel. Figure 14 shows how large vortices are shed as air moves over two obstacles, how these vortices interact downstream with the existing boundary layer, and how boundary-layer material moves away from the wall and is transported out of the system. From this type of computation, we have collected very fundamental information about how boundary-layer material is affected by and interacts with vortices. This is general flow physics that is important for a broad category of flows ranging from flow over riblets, used for cooling on airplane wings, to flow of contaminants through cities.

Just as important, however, understanding this calculation requires understanding how this complex fluid-dynamics simulation differs from the standard diffusion (or “plume”) models used to compute such flows. Figure 15, which compares results of a simulation (such as shown in Fig. 13) to several calculations that use plume models, shows that the results are quite different. At an early time, the plume models predict too much spreading. At the later time, they predict too little. The important lesson here is that you cannot generally equate diffusion, which is the basis for the plume models, with convection, which describes fluid dynamics.



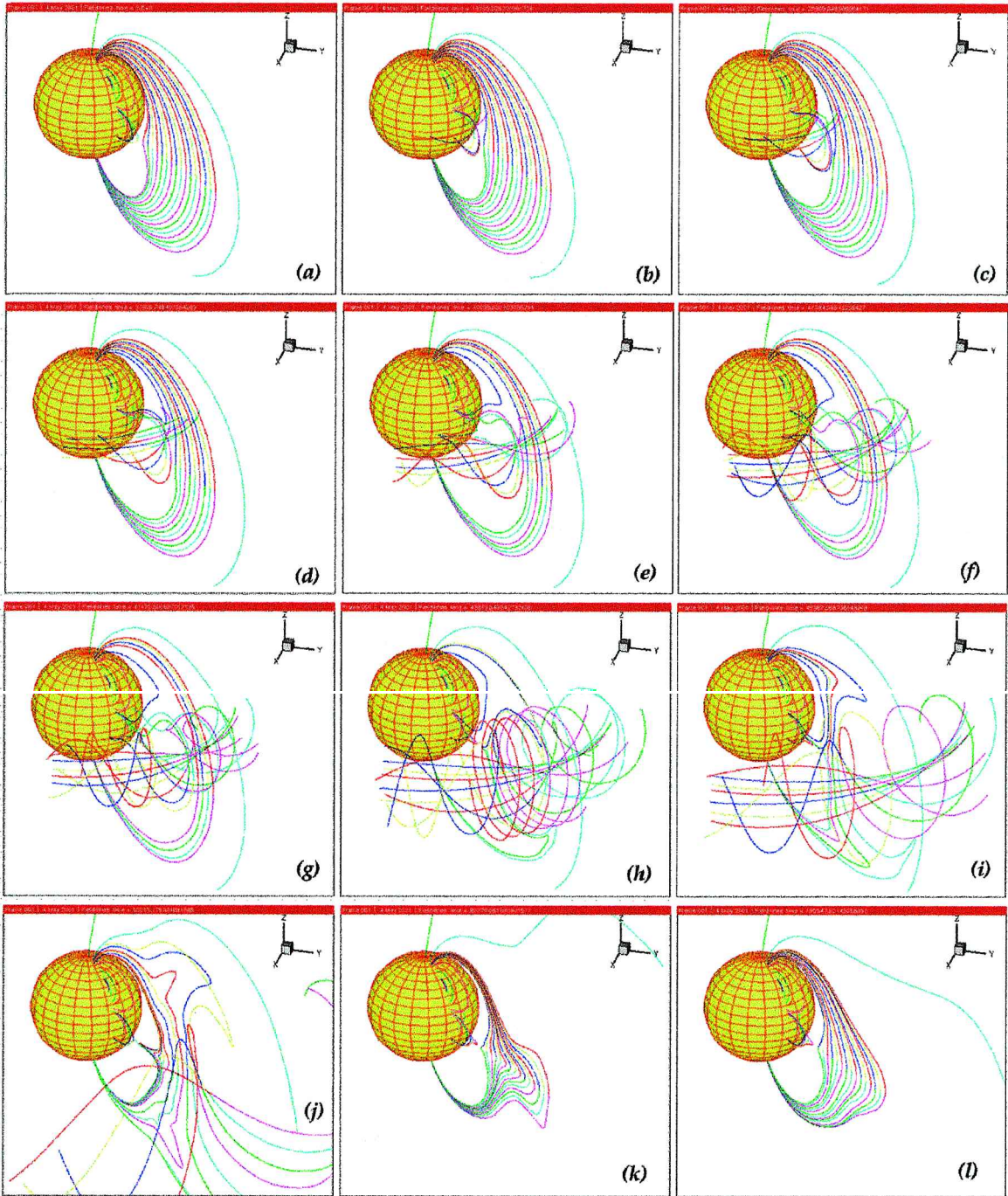


**Fig. 12** Three-dimensional simulations of a coronal mass ejection and eruptive flare.<sup>15</sup> Problem initiated with a) unstressed quadrupolar magnetic field at equator, and at later times b) 18,103 s, c) 29,910 s, d) 37,609 s, e) 40,037 s, f) 41,084 s, g) 41,470 s, h) 45,367 s, i) 48,674 s, j) 50,215 s, k) 60,770 s, and l) 195,548 s.

**Fluid Dynamics with Fast Energy Release**

Fluid dynamics with fast energy release generally describes types of physics common to propulsion, combustion, fires, engines, explosives, weapons, stars, supernovas, and ultimately the formation of the universe. Fires and explosions, which seem to be tremendous sources of loss, may be the result of catastrophic events (so apparent after the events of this past year). They may also be useful, constructive, or a natural part of the environment.

Sometimes the effects of the interactions between fluid dynamics and fast energy release are catastrophic in the sense that they are triggered by events seemingly insignificant on the scale of their results. For example, ignition events are typical of this type of catastrophe: They are extremely complex, involving complicated flows, usually turbulent, coupled to series of complicated, multi-step chemical reactions, and involve multiphase effects. When the

problems are so complex, we often need to stand back and look at common physical elements of the processes, elements that reappear from situation to situation. Examples of this approach are the computational studies of turbulent diffusion flames (e.g., Ref. 7), turbulent flames leading to detonations (e.g., Ref. 8), and soot production (e.g., Ref. 9). These are the types of fundamental computations that provide insight to many different types of real-life scenarios.

We have done extensive numerical simulations to decipher how one of the most dramatic combustion events occurs, the deflagration-to-detonation transition (DDT). (See, for example, Refs. 8, 18, and 19.) In the generic problem, a deflagration, which is a subsonic reaction wave driven by energy release and diffusion processes, changes into a detonation, which is a powerful supersonic shock wave driven by fast energy release behind it. The difficulties of such



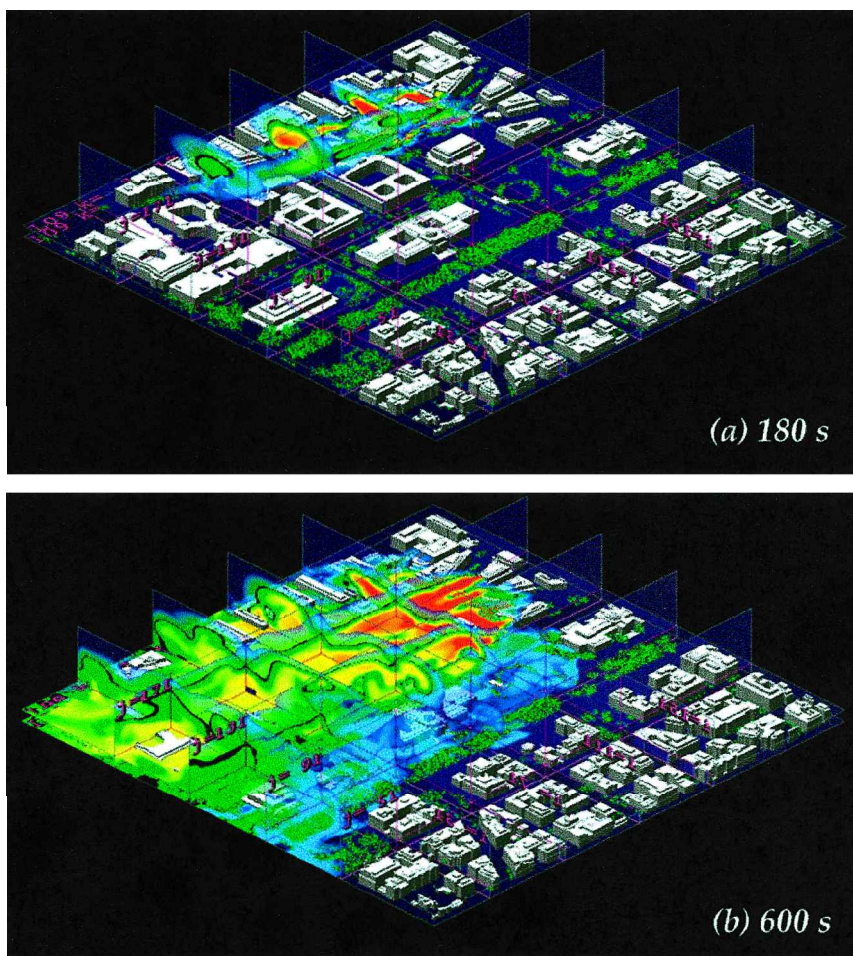


Fig. 13 Simulation of the flow of a contaminant through an urban area similar to the Washington Mall.<sup>17</sup> Instantaneous distribution of the contaminant is shown for a continuous source driven by 3-m/s winds from the east. The distribution is shown either on the plane 2.5 m above the ground level or on one of the vertical planes, depending on which is maximum. View is from the southwest. Colors are the mass density of the agent. Colors run from blue (low density) to green to yellow to red (high density), in a logarithmic scale covering eight orders of magnitude. Zero density is translucent. Black contours indicate that a dangerous level has accumulated.

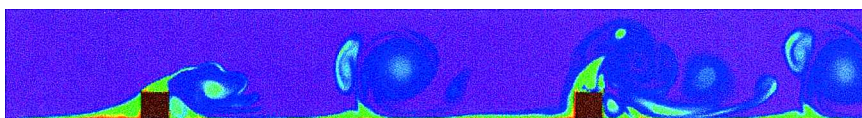


Fig. 14 Viscous, slow (Mach number 0.012) flow from left to right over two riblets. Bottom walls are a few degrees warmer than inflow (X. Saint-Martin Tillet and E. S. Oran, 1996, unpublished). Symmetry boundary at top. Flow over riblets generates vortices that interact with boundary-layer material, separating it from the wall and allowing it to flow out of the system. Colors indicate temperature variations.

calculations arise from the disparity in timescales on which flames and detonations propagate, complicated flow structures on spatial scales ranging from the size of the system to the thickness of a flame, complex chemical, atomic, nuclear, or multiphase reactions, and electromagnetic radiation.

Finding a path through the morass of confusing and often contradictory evidence is a challenge, and we have had some limited successes. Here it has helped to focus on experiments, and we considered the rather simple interaction of a flame and a shock and how it evolves into a turbulent flame, and then how the system may undergo a transition to a detonation. Figure 16 is a composite of frames taken from a simulation in which a shock hits a flame, shock-flame interactions result in a turbulent flame, and eventually a detonation emerges “spontaneously” from the system.<sup>8</sup> Subsequent computations have clarified the role of differences between two and three dimensions, the role of boundary layers, and, most recently, the role of wakes. Yet to be studied, but extremely important and not to be overlooked (!), are the effects of complex, multistep energy-releasing reactions and multiphase effects.

One more point should be made here. This is the type of problem for which three-dimensional computations, even when they can be

done, could be more confusing than helpful in understanding the problem. Figure 17 shows a series of frames taken from a computation of a similar situation to that shown in Fig. 16, but for a three-dimensional system. This computation shows all of the flow physics and boundary-layer interactions that Fig. 16 shows. Yet without having seen and studied the dynamic events in two dimensions, three-dimensional simulations would be close to unintelligible.

These are also tour de force computations that required extensive computational resources and new algorithms. Whereas the boundaries and geometry of a computation such as that shown in Fig. 17 are not that complicated, the flow structures that develop are extremely complicated. Six years ago, we estimated that it would take a year of computer time to perform the computation shown in Fig. 16. Today, with dynamic and adaptive regridding, this computation can be done and interpreted in days.

Now we bring the problem full circle. The general importance of rather basic studies, such as shown here, is a theme that runs through this paper. It is studies such as that shown in Fig. 16, when applied to flames and detonation in thermonuclear systems, that are likely to give us the answer to the question of how supernova explosions shown in Fig. 11 detonate.

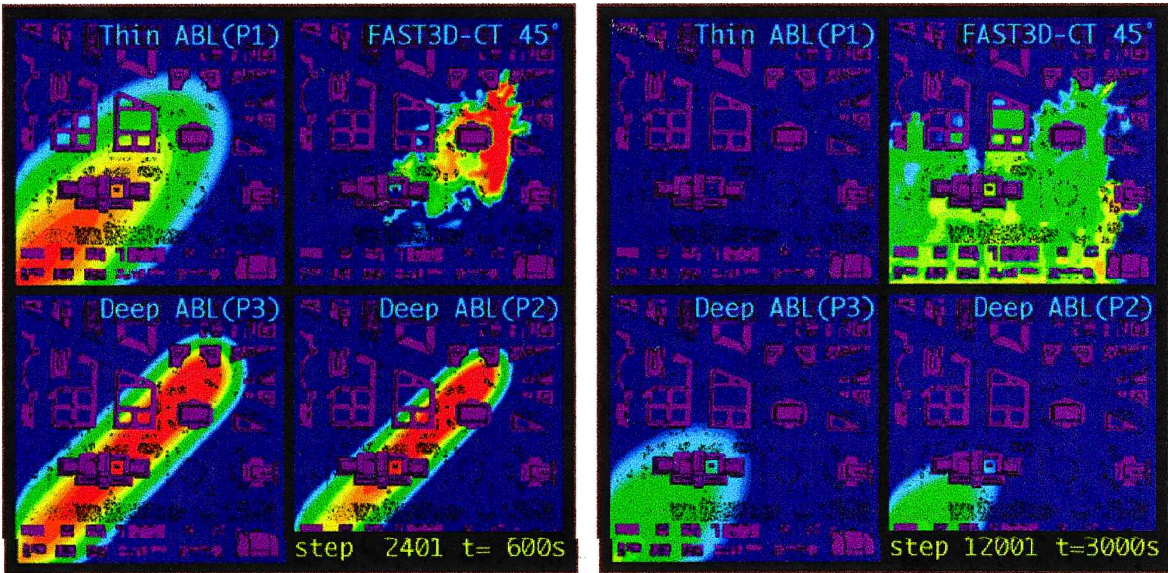


**Fig. 15** Comparison of a computation, similar to that shown in Fig. 4, to computations performed with three different types of Gaussian similarity solution (basis of plume models).<sup>17</sup> Thin atmospheric boundary layer (ABL), such as in a field or the desert, are labeled P1. Deep ABLs (P2) and (P3) are thicker, more typical of urban areas. Deep ABL (P3) indicates a larger diffusion coefficient, which is another variable in plume models. The computation marked FAST3D-CT was performed by solving the fluid continuity equations, especially designed to compute cases of contaminant transport.

Table 2 Levels of models of many-body interactions	
Equation	Solution method
String theory, quantum gravity? relativity?	
Field theories (QCD, EW, SUSY)	
Schrödinger's equation	Direct solution, density functional theory, (prescribed interparticle forces)
Newton's law $f = ma$	Molecular dynamics (particle-based, prescribed interparticle forces)
Liouville equation	Monte Carlo methods
Equation for distribution function, $F(x_i, v_i, t), i = 1, N_p$	(statistical, particle-based methods)
Boltzmann equation $F(x, v, t)$	Direct simulation Monte Carlo
Binary collisions (low density)	Direct solution
Good for gases	
Generalized continuity equation: Navier-Stokes equation and MHD	
$\rho(x, t), u(x, t)$	Direct solution: finite differences, finite volumes, spectral methods, etc. (continuum flow methods)
Short mean free path	
Equations of general relativity	

**V. When These Equations Break Down . . .**

Table 2 shows the hierarchy of mathematical models used to describe the behavior of systems involving many particles and interactions. The computations discussed in Figs. 1–17 are all solutions of continuum equations based on generalizations of the Navier–Stokes equations, which can be expressed in the form of the generalized continuity equation. Even though such solutions appear to be a relatively small subset of physics in Table 2, we already know the breadth of what they can represent. Now consider what happens when the basic assumptions that lead to this continuity equation break down. We still require whatever model we use to be constrained by causality and conservation laws, but certain other assumptions may no longer hold.

When there are too few molecular collisions, we can no longer assume that material can be represented as a continuum, and we need to consider the behavior of collections of particles explicitly. (This is moving up in Table 2 with respect to where the Navier–Stokes

equations are located.) Examples of this are when extraterrestrial objects, such as asteroids, comets, and meteors, or man-made space vehicles enter the atmosphere.

Consider the problem of reentry of the Mir Space Station into the Earth’s atmosphere. This occurred at least partially in a low-density region of the atmosphere, where there are too few collisions to achieve fluid equilibrium. To reenter in the safest possible. Also, the drag should be maximized, in order to burn up as much of the vehicle as possible. Also, the stress on parts of the vehicle should be minimized, so that it does not break into many large parts. Results of computations<sup>20</sup> of Mir reentry are shown in Fig. 18.

Another example, shown in Fig. 19, is the flow in a microfilter,<sup>21,22</sup> a gaseous component of a microfluidic microelectromechanicals system (MEMS) device. Such a component may be part of an air-intake section of a sensor system that tests for pathogen or pollutants. Here the density is much higher than in the Earth’s upper atmosphere, but nonequilibrium effects become very important because the characteristic sizes of microfilters will go down to less than 1  $\mu\text{m}$ . These conditions again lead to a situation in which there are too few collisions to achieve fluid equilibrium.

The Mir spacecraft has characteristic size scales on the order of meters, and the density is low. The MEMS microfilter has size scales on the order of micrometers, and the density is much higher. Even though these systems differ in size by many orders of magnitude, they have this fundamental physical similarity: There are too few molecular collisions to attain equilibrium. The ratio of the mean free path of the particles to a characteristic scale length of the system, a quantity called the Knudsen number, is too high for us to be able to assume continuum fluid behavior. The behavior of both of these flows, in what is called the transition regime of fluid equilibrium, has been computed using the particle-based method, direct simulation Monte Carlo, which, as shown in Table 2, is a way of solving the Boltzmann or Liouville equations for many-particle interactions.

Another example of when the basic form of the continuity equations does not hold is when bodies are very massive or move very fast, so that Newtonian mechanics breaks down. Then we need to consider relativistic effects. (This is moving down in Table 2.) Examples here include relativistic particle beams or black holes. Relativistic particle beams can be modeled using the equations of special relativity: The particles move very fast, but they are not that massive. These equations are also generalizations of the generalized continuity equation, now with additional special constraints on variables to ensure that nothing moves faster than the speed of light.



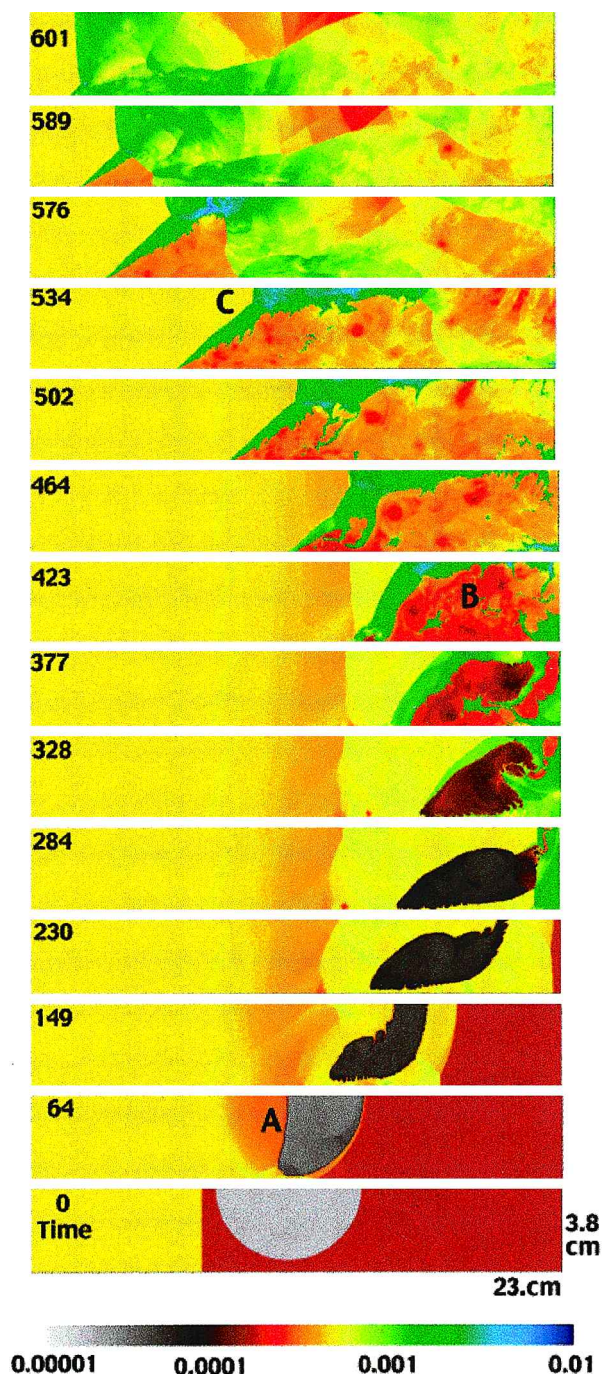


Fig. 16 Density maps taken from a simulation in which a flame is created by a spark in the center of a system, a shock hits the flame and shock-flame interactions result in a turbulent flame, shocks and flames interact with boundary layers, and eventually a detonation emerges in the system.<sup>8</sup> Simulation is unsteady, two dimensional, of lower half of the system (symmetry boundary along top of computational domain). Solution of the Navier-Stokes equations with a model for energy release, molecular diffusion, thermal conduction, viscosity, calibrated for a stoichiometric ethylene-air mixture. Unperturbed background initially at 100 torr and 298 K: A) shock-flame interactions, B) turbulent flame forms, and C) DDT. Time shown in upper left corner of each frame, measured in microseconds. Density scale in  $\text{g/cm}^3$  shown at bottom.

No such simplifications exist for black holes and black-hole interactions. These require solving the equations of general relativity because their strong gravitational effects distort space-time. Currently there is a concerted international effort to solve these equations for the case of black holes merging, perhaps one of the strangest astrophysical events we can consider today. This effort is driven by the expected flight of instruments that should be able to measure the gravitational wave spectrum generated by such

strong space-time events. Figure 20 is based on a simulation performed by the Lazarus group (Max Planck Institute for Gravitational Physics) of two black holes spiraling into each other.<sup>23</sup> For this problem, solution techniques are several years away from reaching the stage where we can do a complete, direct solution of Einstein equations for the entire process. The major advance made by this group is to develop a hybrid of several approaches, each appropriate for different regimes of the merging process. Only the most dynamic and strongest interaction, the final approach of two black holes, is solved using the full set of equations. Two different forms of perturbation theory are used to describe the initial, gradual approach of the objects and the final settling down after merging.

A last type of example does not fit neatly into the list in Table 2. It is what occurs when the effects of very different space or timescales do not average out on the larger scale. This is an effect we sometimes call “leakage,” and it has recently received attention under the rubric of “multiphysics.” Leakage between vastly different scales is what creates the unusual processes we see in non-Newtonian flows, such as polymer solutions, foams, slurries, or blood. In these cases, it is usually hard to even know what the physical model should be, let alone how to simulate the behavior of the system.

For example, suppose we introduce a very small amount of a certain polymer into a normal, Newtonian fluid such as water. The result we would expect in a Newtonian fluid is that the viscosity of the mixture should be slightly higher, but essentially unchanged. The result, however, for certain polymers is that the material behaves as if the viscosity were much lower. This phenomenon is not really understood, but its explanation lies in understanding the behavior of long chains of molecules that take a relatively long time to unravel and ravel in the water. In these cases, the molecular properties of a minor constituent in the fluid are having a strong effect on the macroscopic, continuum properties of the major constituent. The behavior of such non-Newtonian fluids might be modeled by modifying selected terms in the governing equations, or it might be modeled by a molecular-dynamics approach that describes the behavior of the long-chain molecules and their interactions with the small water molecules or clusters, or it might be modeled by a hybrid fluid-particle model. This is a current forefront of computational research on non-Newtonian flows.

## VI. Enabling Technology

A two-dimensional computation with  $10^6$  computational cells was considered very large 15 years ago. Assumptions of steady state were the best that could be done for many systems. Today, three-dimensional computations with true dynamics have been performed with more than  $10^9$  computational cells. Complex, time-dependent simulations, that were considered an esoteric art confined to a few laboratories with large computers, can now be readily solved by most scientists and engineers on their desktop workstations. All of this reflects continuing exponential advances in computer memory and computational speed.

Figure 21 qualitatively illustrates these advances in computer speed and memory as a function of year (based on updating a lecture by Worlton<sup>24</sup>). The essentially straight line increase of overall performance on the semilog scale means that computer power and memory is scaling exponentially. Our projections, based on the current understanding of technology, are that this rate can hold for at least another 10 years. Figure 21 shows that the exponential performance increase is really composed of a series of piecewise logistic curves, each representing the introduction of a new technology. The result of adding all of the curves is sustained exponential growth. For example, early breakthroughs have included introducing transistors to replace vacuum tubes and semiconductor memory to replace magnetic cores. More recently, we have changed from scalar to vector architectures and from serial to parallel computing. Such a curve is typical of the growth of an enabling technology, such as high-performance computing. The continuous improvement of each component technology saturates and levels out at some point because the particular technology that allowed the growth becomes



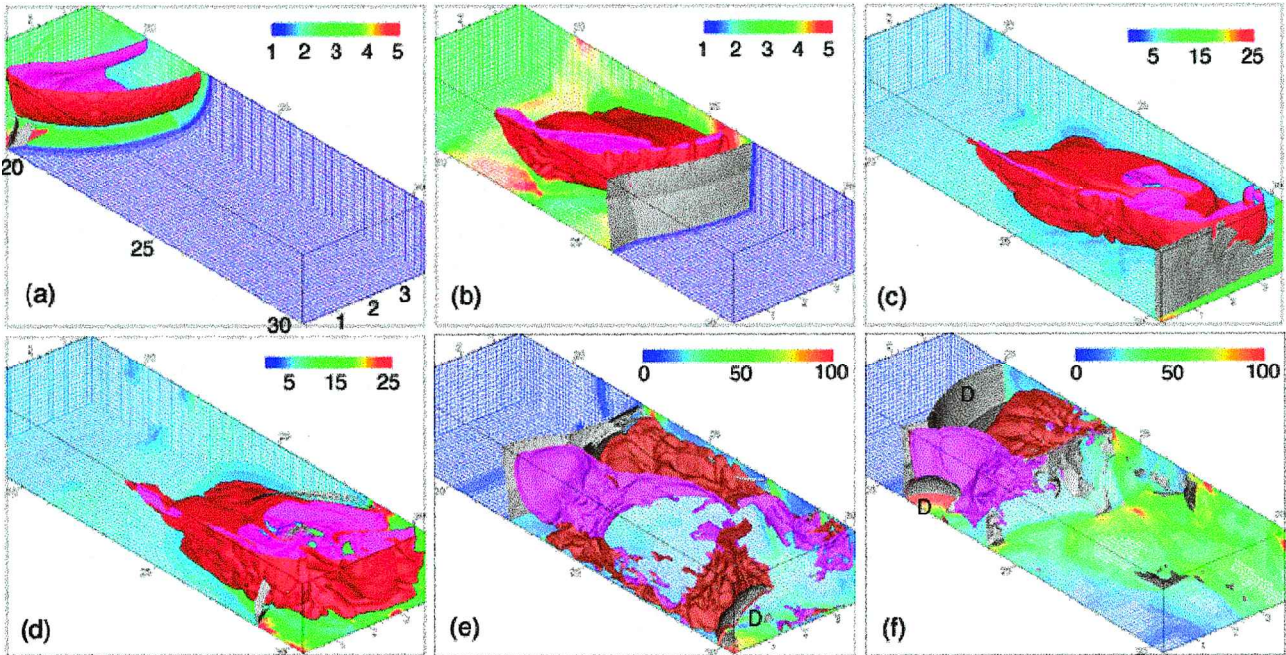


Fig. 17 Sequence of frames showing normalized pressure ( $P/P_0$ , where  $P_0$  is the initial background pressure) from three-dimensional simulations of the system shown in Fig. 6. The initial flame is now spherical. Frames show bottom quarter of the system from perspective of reflecting wall: a)  $78\ \mu\text{s}$ , the incident shock is partially through the flame; b)  $168\ \mu\text{s}$ , the shock has fully emerged from the flame and is moving toward the reflecting back wall (toward the viewer); c)  $248\ \mu\text{s}$ , the shock is just reflecting from back wall, the turbulent flame is developing; d)  $304\ \mu\text{s}$ , the shock is moving back through the distorted, turbulent flame; e)  $370\ \mu\text{s}$ , the emergence of a detonation  $D$  in the region near the back wall; and f)  $476\ \mu\text{s}$ , the emergence of detonations. (Calculation by Gamezo et al.)

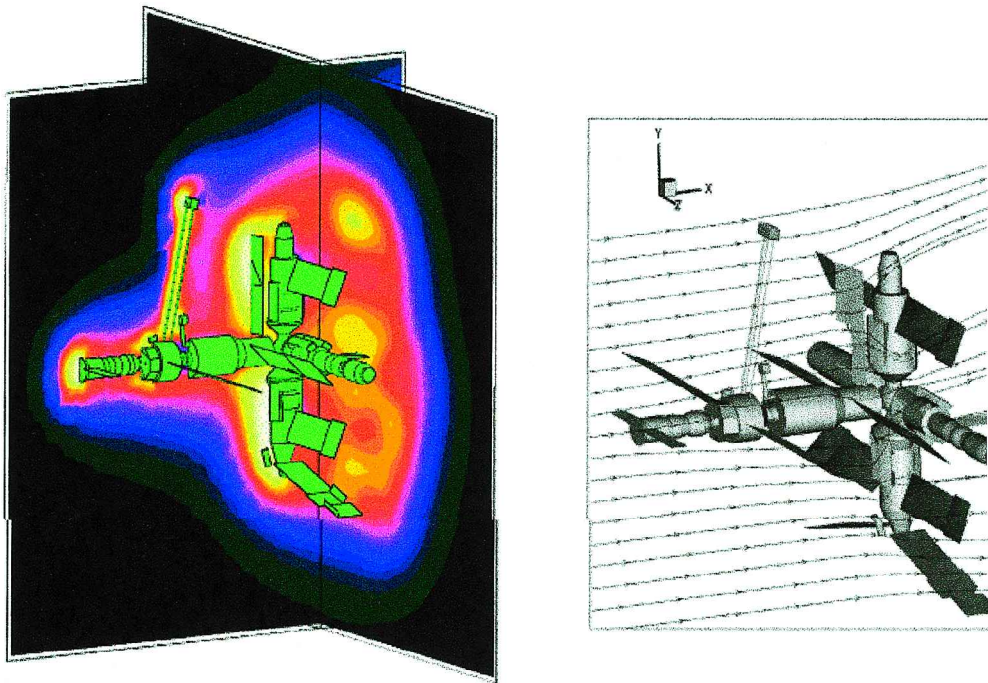


Fig. 18 Pressure (left) and velocity vectors (right) for the flow over the Mir Space Station at 110 km (Ref. 20). The physical scale, about 10 m, and the low density of the upper atmosphere, about  $10^8\ \text{kg/m}^3$ , put this problem in a range where the fluid dynamics is not equilibrated, and particle-based methods give more accurate solutions.

too expensive and time consuming to improve. One obvious, and in some ways alarming, feature of this curve is that to continue the growth and not stagnate, new technologies must regularly be discovered.

Along with the development of high-end computing, there have been improvements in personal computers and desktop workstations. As hardware and software become more sophisticated, computing improved in every way. Currently, most parallel supercomputers have about the same speed per processor because they

are based on the same or similar chips. The performance increases are driven by microprocessor technology rather than research and development aimed at supercomputer architectures.

The current design philosophy tends to use the same basic components (chips) for both supercomputers and powerful workstations. This philosophy may slow the overall pace of computer development because the high-end systems are less and less the drivers of new technology. Alternately, it could speed the pace because there is broad-based public demand for faster desktop computing.



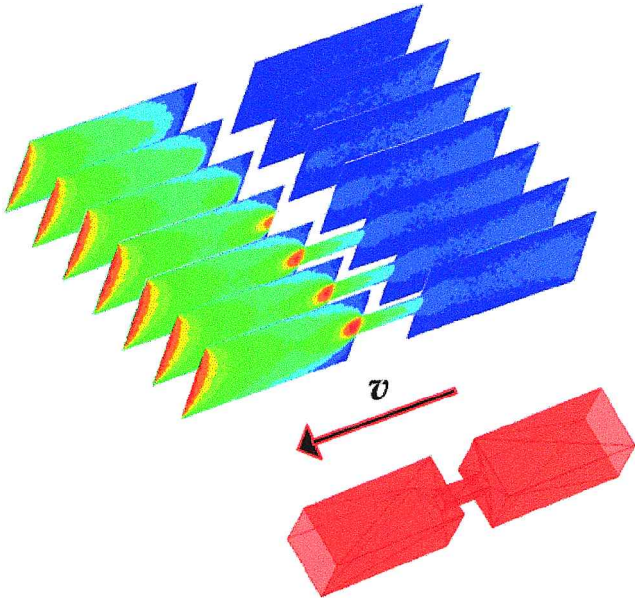


Fig. 19 Frames from a three-dimensional simulation of a gaseous microfilter.<sup>22</sup> Physical scale size is about  $10^{-6}$  m, and low density of the upper atmosphere, about  $0.1 \text{ kg/m}^3$ , puts this problem in a range where the fluid dynamics is not equilibrated, and particle-based methods give more accurate solutions.

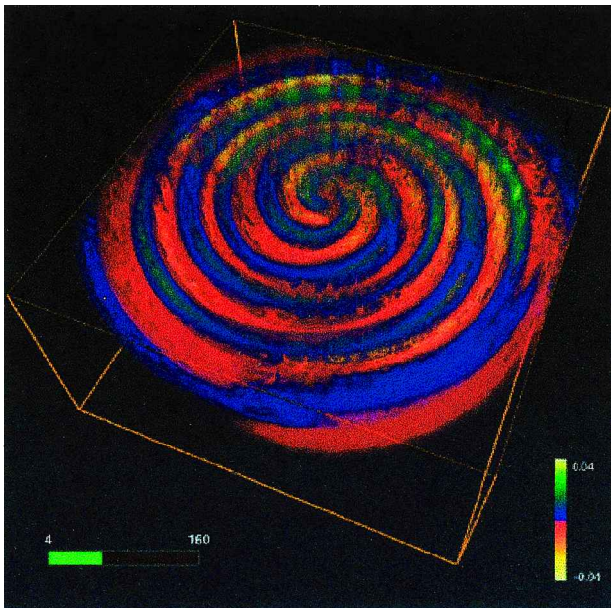


Fig. 20 Frame showing the gravitational wave spectrum from the inward spiral of two black holes.<sup>23</sup> This simulation was performed by the Numerical Simulation Group at the Max Planck Institute for Gravitational Physics (Golm, Germany), and visualizations were created by Werner Benger with the Amira software at the Konrad Zuse Zentrum für Informationstechnik (Berlin, Germany), Department of Scientific Visualization.

This is a curious interplay that has practical consequences for scientific computing. Figure 22 summarizes recent trends in the computers by showing the megahertz per processor rating as a function of the number of processors for several of the largest computers available. The graph shows that the current maximum processor speed is 1 or 2 GHz, and that is what we can commonly get on our desktops.

High-end computers differ in their interprocessor communications, memory structure, and architectures. The memory may be globally shared or distributed among the processors. Interprocessor communications may or may not scale linearly as a system expands from a few processors to many processors, and various problems can arise in sending data among processors. At another

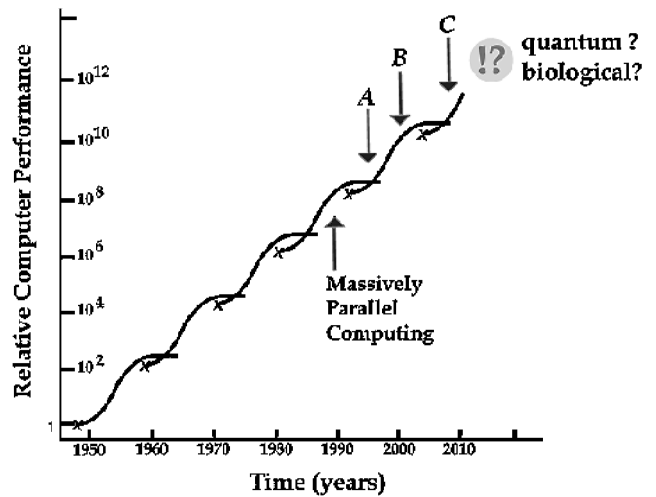


Fig. 21 Computer technology. By 2015, we will need to invent something new in computing. A indicates simplest calculation shown in this paper, B most complex problem, and C next level of complexity and next level of problems, with teraFLOPS regularly accessible and 10 gigaFLOPS on the desktop (?).

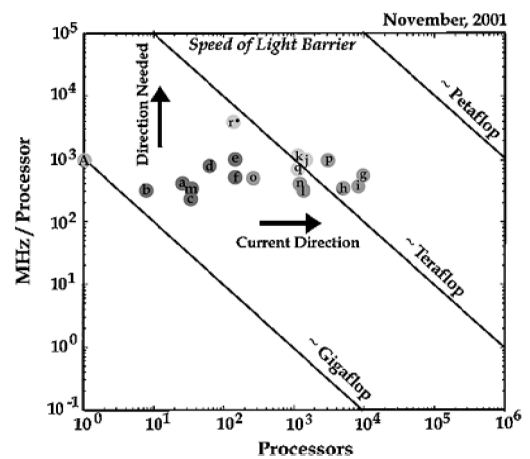


Fig. 22 Graph of megahertz per processor vs number of processors available on some of the largest existing computers, in November 2001. Circles are selected computers as described on the website, VPPP5000, World's Fastest Supercomputers (<http://www.top500.org/list/2001/11/>). The speed of light barrier is estimated based on connectivity times on a computer chip, using current silicon-based technology. The lines indicating gigaFLOPS, teraFLOPS, and petaFLOPS are estimates to within a factor of  $\pm 2$ .

level, the different architectures cause problems in moving computer programs from one type of machine to another (the "portability" problem). The current goal is to obtain computational speeds of many teraFLOPS ( $10^{12}$  floating-point operations per second), whereas computers delivering many gigaFLOPS ( $10^9$  floating-point operations per second) are becoming common. Figure 22 shows that we are increasing computational speed by adding processors, and this is the approach to attaining speeds of teraFLOPS or petaFLOPS. This is somewhat different from what this graph looked like 10 years ago, when developments were taking every direction and there were no clear trends except the drive toward bigger and faster.

It is interesting to ask the extent to which the requirements of simulations such as those discussed in this paper, which span many disciplines, drive the development of high-end computing. This was certainly the case in the "early days," before there was a personal computer or two on everyone's desk at home. In that period, for example, government funding ensured that there would be newer, larger, faster, and more different types of computers available to deal with major problems in national security and defense. Now, economics and industrial competition are what is driving the development of newer, smaller, and faster electronic components, with

defense and security issues only a part of the equation. This is part of the explanation for the trend toward building computers with many coupled smaller processors, with components that were developed originally for the large market calling for faster, smaller personal computers.

Figure 21 makes the alarming point that by approximately 2015, we will need to invent something new in computing to stay on this exponential curve. What exactly it will be is far from certain, though there is a good chance that we will be moving away from silicon-based components. There are now substantial, even brilliant efforts in quantum computing that could provide the basis for a revolution in information storage and transmission, and so in very basic ways of how computers work. Quantum computers could be a reality in 10 years.

## VII. Summary and Concluding Remarks

What have we learned and where are we, after all of the work of the past 30 years?

1) We see that numerical simulation of real problems requires combining knowledge and methods from many disciplines of science, mathematics, and engineering.

2) We see that much of the algorithmic advances are due to the fact that there are useful similarities in the underlying forms of the governing equations (... because the equations are based on conservation laws).

3) We understand the importance of fundamental processes in the most complicated systems.

4) By simulating such a wide range of physical systems, we have learned how to deal efficiently with a wide variety of complexities in physics and geometry.

5) We are learning to deal with problems for which basic continuum, equilibrium assumptions break down.

So that now,

6) Simulations of complex flows are pushing the limits of computer science and technology.

7) There is enormous flexibility as to what we simulate. We should be thinking of going "beyond nature" for design, basic knowledge, and even curiosity.

Now let us examine this last point.

With the computational power we have today, an enormous amount has been done in terms of the variety of complex flows we are simulating. We have seen very practical simulations performed for purposes of design and danger assessment and other calculations done to increase our understanding of how the world and universe work.

However, if we so desire, we might even now go beyond nature. We might consider going beyond nature to design undersea craft as graceful and efficient as manta rays, to improve the design of the human body, to terraform other planets, or to create smart, organic structures in which to live and work. We might consider going beyond nature to control or redesign plate tectonics, volcanic eruptions, the human circulatory system, or gravity. For perverse curiosity, we can even compute the consequences of 4, 5, 11, or 21 spatial dimensions, or imagine a black-hole trash compactor that generates the energy needed to operate it, or even how to use a black hole for propulsion!

## Acknowledgments

Funding for the work presented here was from the Office of Naval Research through the Naval Research Laboratory, the Defense Advanced Research Projects Agency, NASA, the U.S. Air Force, and the Department of Defense High-Performance Computing Modernization Office. I would like to thank many friends and colleagues for their contributions to the technical materials and discussions underlying what was presented in this paper. In particular, I would like to Jay P. Boris, Bernd Brüggemann, C. Richard DeVore, Kozo Fujii, Vadim N. Gamezo, Mikhail Ivanov, Carolyn R. Kaplan, David R. Mott, David Fyfe, Alexei M. Khokhlov, Ravi Ramamurthi, Fernando Grinstein, Theodore Young Jr., and Kazuhiro Nakahashi. Some of the text in this article is a variation and update on that published with Jay Boris in Ref. 2, *Numerical Simulation of Reactive Flow* (2nd edition). The advice, discussion, and encouragement from Daniel H. Oran, Elizabeth T. Boris, and Marlowe M. Brown were critical

to the organization and presentation of the material. I am grateful to Keith Obenshain and Kevin Harris for their help preparing the visualizations and for technical aspects of the presentation. Finally, I would like to thank C. Richard DeVore, David R. Mott, Carolyn R. Kaplan, and Rowena Ball for reading and commenting on this paper.

## References

- Gorn, M. H., "Hugh L. Dryden's Career in Aviation and Space," NASA Monographs in Aerospace History, No. 5, 1996.
- Oran, E. S., and Boris, J. P., *Numerical Simulation of Reactive Flow*, 2nd ed., Cambridge Univ. Press, New York, 2001.
- Sandberg, W. C., Ramamurti, R., Löhner, R., Walker, J. A., and Westneat, M. M., "Pectoral Fin Flapping with and without Deformations in the Bird Wrasse; 3-D Unsteady Computational," *Journal of Experimental Biology* (submitted for publication).
- Ramamurti, R., Sandberg, W. C., and Löhner, R., "Simulation of a Torpedo Launch Using a Three-Dimensional Incompressible Finite-Element Solver and Adaptive Remeshing," AIAA Paper 95-0086, 1995.
- Landsberg, A. M., Boris, J. P., Sandberg, W. C., and Young, T. R., Jr., "Analysis of the Nonlinear Coupling of a Helicopter Downwash with an Unsteady Airwake," AIAA Paper 95-0047, 1995.
- Fujii, K., and Ogawa, T., "What Have We Learned from Computational Fluid Dynamics Research on Train Aerodynamics?," *Frontiers of Computational Fluid Dynamics 1998*, edited by D. Caughey and M. Hafez, World Scientific, Singapore, 1998, pp. 401-421.
- Grinstein, F., "Vortex Dynamics and Entrainment in Rectangular Free Jets," *Journal of Fluid Dynamics*, Vol. 473, 2001, pp. 69-101.
- Gamezo, V. N., Khokhlov, A. M., and Oran, E. S., "The Influence of Shock Bifurcations on Shock-Flame Interactions and DDT," *Combustion and Flame*, Vol. 126, 2001, pp. 1810-1826.
- Kaplan, C. R., Shaddix, C. R., and Smyth, K. C., "Enhanced Soot Production in Time-Varying CH<sub>4</sub>/Air Diffusion Flames," *Combustion and Flame*, Vol. 106, No. 4, 1996, pp. 392-405.
- Togashi, F., Ito, Y., Murayama, M., Nakahashi, K., and Kato, T., "Flow Simulation of Flapping Wings of an Insect Using Overset Unstructured Grid," AIAA Paper 2001-2619, 2001.
- Cybyk, B. Z., Boris, J. P., Young, T. R., Lind, C. A., and Landsberg, A. M., "A Detailed Contaminant Transport Model for Facility Hazard Assessment in Urban Areas," AIAA Paper 99-3441, 1999.
- Teramoto, T., Hiraki, K., and Fujii, K., "Numerical Analysis of Dynamic Stability of a Reentry Capsule at Transonic Speeds," *AIAA Journal*, Vol. 39, No. 5, 2001, pp. 646-653.
- Antiochos, S. K., DeVore, C. R., and Klimchuk, J. A., "A Model for Solar Coronal Mass Ejections," *Astrophysical Journal*, Vol. 510, Jan. 1999, pp. 485-493.
- Gamezo, V. N., Khokhlov, A. M., and Oran, E. S., "Three-dimensional Numerical Simulations of Thermonuclear Supernovae," *Astrophysical Journal* (submitted for publication).
- Antiochos, S. K., MacNeice, P. J., and DeVore, C. R., "Formation of Magnetic Clouds in Eruptions of Sheared Coronal Arcades," *Astrophysical Journal* (submitted for publication).
- Cybyk, B. Z., Boris, J. P., Young, T. R., Emery, M. H., and Cheatham, S. A., "Simulation of Fluid Dynamics around Complex Urban Geometries," AIAA Paper 2001-0803, 2001.
- Boris, J., "The Threat of Chemical and Biological Terrorism: Roles for HPC in Preparing a Response," *IEEE Computing in Science and Engineering*, March/April 2002, pp. 22-32.
- Khokhlov, A. M., and Oran, E. S., "Numerical Simulation of Detonation Initiation in a Flame Brush: The Role of Hot Spots," *Combustion and Flame*, Vol. 119, No. 4, 1999, pp. 400-416.
- Oran, E. S., Gamezo, V. N., and Khokhlov, A. M., "Effects of Boundary Layers and Wakes on Shock-Flame Interactions and DDT," AIAA Paper 2002-0776, 2002.
- Markelov, G. N., Kashkovsky, A. V., and Ivanov, M. S., "Space Station Mir Aerodynamics Along the Descent Trajectory," *Journal of Spacecraft and Rockets*, Vol. 38, No. 1, 2001, pp. 43-50.
- Mott, D. R., Oran, E. S., and Kaplan, C. R., "Microfilter Simulations and Scaling Laws," *Journal of Thermophysics and Heat Transfer*, Vol. 15, No. 4, 2001, pp. 473-477.
- Kaplan, C. R., Mott, D. R., and Oran, E. S., "Scaling Laws from 3D Microfilter Simulations," *Proceedings of the 23rd Rarefied Gas Dynamics Conference* (to be published).
- Baker, J., Brüggemann, B., Campanelli, M., Lousto, C. O., and Takahashi, R., "Plunge Waveforms from Inspiral Binary Black Holes," *Physical Review Letters*, Vol. 87, No. 12, 2001, pp. 121103-1-121103-4.
- Worlton, J., "Some Patterns of Technological Change in High-Performance Computers," *Proceedings of Supercomputing '88*, IEEE Computing Society Press, Washington, DC, 1988, pp. 312-320.